World Electric Vehicle Journal

MDPI

Article

Effects of the Incorporation of Electric Vehicles on Protection Coordination in Microgrids

Sergio D. Saldarriaga-Zuluaga [1,*], Jesús M. López-Lezama [2], Carlos David Zuluaga Ríos [1] and Alejandro Villa Jaramillo [1]

[1] Departamento de Eléctrica, Facultad de Ingenieria, Institución Universitaria Pascual Bravo, Calle 73 No. 73A-226, Medellín 050036, Colombia
[2] Research Group on Efficient Energy Management (GIMEL), Departamento de Ingeniería Eléctrica, Universidad de Antioquia (UdeA), Calle 70 No. 52-21, Medellín 050010, Colombia
* Correspondence: s.saldarriagazu@pascualbravo.edu.co

Abstract: Amid growing concerns about climate change, electricity-powered transportation systems stand out as an opportunity to help in reducing fuel consumption. Electric vehicles (EVs) would connect to the grid using clean, renewable electricity; however, the interconnection between EVs and the grid brings about new challenges for traditional power systems. Plug-in hybrid EVs and plug-in EVs have started to become more prevalent in the system; therefore, their impacts and benefits are also of concern. Among these concerns is the detailed analysis of the impact that EVs may have on short-circuit levels in microgrid protection schemes. In this context, the main contribution of this paper is a detailed evaluation of the impact of EVs on the short-circuit levels and protection coordination schemes in microgrids. For this purpose, a methodology was proposed to measure the impact of EVs on the protection coordination schemes in microgrids using different evaluation indices. The proposed approach was validated on a benchmark IEC microgrid considering different operative scenarios that envisage several levels of EVs penetration. The results evidenced the applicability of the proposed approach and allows to conclude that the incorporation of EVs in microgids impacts the performance of the protection schemes, specifically with respect to short-circuit levels.

Keywords: electric vehicles; microgrids; overcurrent relays; protection systems

check for updates

Citation: Saldarriaga-Zuluaga, S.D.; López-Lezama, J.M.; Zuluaga Ríos, C.D.; Villa Jaramillo, A. Effects of the Incorporation of Electric Vehicles on Protection Coordination in Microgrids. *World Electr. Veh. J.* **2022**, *13*, 163. https://doi.org/10.3390/wevj13090163

Academic Editor: Joeri Van Mierlo

Received: 26 July 2022
Accepted: 19 August 2022
Published: 29 August 2022

Publisher's Note: MDPI stays neutral with regard to jurisdictional claims in published maps and institutional affiliations.

Copyright: © 2022 by the authors. Licensee MDPI, Basel, Switzerland. This article is an open access article distributed under the terms and conditions of the Creative Commons Attribution (CC BY) license (https://creativecommons.org/licenses/by/4.0/).

1. Introduction

Amid growing concerns regarding climate change, key government and private sector stakeholders have pushed to move away from oil as the primary energy source to power transportation systems. Electricity-powered transportation systems allow reducing oil consumption. In this context, electric vehicles (EVs) can be connected to the grid, and their on-board battery system can be recharged using clean, renewable electricity [1].

Beyond the limitations of battery technologies, a key remaining challenge to the widespread adoption of EVs is the lack of a refueling infrastructure for recharging electric vehicle batteries quickly and seamlessly to extend the driving range during long trips. Therefore, there is an urgent need for a charging infrastructure that parallels existing gasoline stations, particularly in regions where long-distance travel is common. However, designing and implementing such a charging infrastructure is complex and must consider the competing industry standards, available technologies, and grid impacts, among other technical and policy issues [2].

Whenever there is an improved interconnection between EVs and the grid, complications will arise for traditional power systems. Plug-in hybrid EVs and plug-in EVs have started to become more prevalent in the system. As the technology matures and customer acceptance increases, the impacts and benefits of EVs becomes of increasing concern. The services that EVs can provide to the existing energy system are quickly becoming a research issue. EVs have the potential to increase the power consumption of the system and overload

the grid; nonetheless, they also represent significant distributed energy storage capacity that can provide services to the grid, even if they are only charging [3].

Chargers can be unidirectional o bidirectional; furthermore, they can be inside or outside the vehicle. Unidirectional charging systems feature simple charging hardware and permits power to flow from the grid to the EV but not vice versa. Bi-directional charging allows power to flow from the grid to the EV and also from the EV to the grid (V2G), building (V2B) or home (V2H) [4]. V2G type charging stations have a greater impact on the distribution network due to their characteristics. There are other charging alternatives such as wireless charging systems which remove the hassle of plugging in the device to be charged. Also, wireless charging is considered to be environment and user friendly as the wires and mechanical connectors as well as other related infrastructure are not required [5].

The large number of EVs accessing the power grid has brought along some complications. The most challenging of these issues are the safety and economics of the power system. One of the most critical issues is the problem of increased power loads due to the connection of EVs to the grid at peak hours, which further increases the gap between supply and demand. The charging routine of EVs and the individual behavior of their owners varies greatly. This randomness makes more difficult to keep the power grid under control and stable, impacting the overall performance of the power grid [6].

Several research studies have been carried out in the technical literature, aiming to analyze and reduce the impacts of EVs on the electric grid. These studies evaluate the impact of EVs on the power grid from different technical aspects: chargeability, voltage stability, harmonics, and variations in short-circuit levels, among others. For example, in [7], the authors evaluate the impact of EVs on the investment and power loses in distribution networks. The authors in [8] present a conceptual framework for successfully integrating EVs into electric power systems. The proposed framework covers two different domains: the technical operation of the grid and the electricity market environment. In [9,10], the influence of EVs charging on power system voltage stability under different scenarios is evaluated. In [11], the authors present a brief review of EVs as well as their effects on the power grid and power quality. A detailed review of the impacts of EVs charging and discharging on the grid is also presented. In [12], the authors present a complete and updated review of EV charging control structure and optimization methodologies for EV charging and discharging management in power systems.

In [13], the authors investigate demand response (DR) programs based on smart plug-in electric vehicle (PEV) charging and discharging to improve distribution system reliability. The authors in [14] evaluate the impact of EVs on increasing short-circuit currents, decreasing voltage levels, and equipment lifetime. A review of the eventual negative impacts of EVs charging on electric power systems, mainly due to uncontrolled charging, is presented in [4]. It is subsequently shown that through controlled charging and discharging, these impacts can be reduced and even be positive for the system. A comprehensive review and analysis on commercial EVs charging is presented in [15]. In [16], the design of a protection scheme for an EV charging station using solar panels is presented. In [17] the authors present an evaluation of EVs in power distribution networks focusing on capacity adaptation of charging stations.

In [18], the authors study the impact of EVs on fault levels. The results obtained show that a high penetration of PHEVs charging from the grid increases the supply and fault currents. In [19], the impacts on distribution systems due to large-scale integration of EVs during fault condition are studied, and it is concluded that the fault location process can be affected. Finally, in [20], a detailed analysis of the contributions of EVs to fault currents is performed, based on the international standards [21–23], considering the actions of battery energy storage systems (BESS) controllers and the characteristics of power electronic converters (PECs).

Changes in short-circuit levels due to the increasing presence of EVs in microgrids may lead to safety and reliability issues; nonetheless, from the bibliographical research carried out by the authors, it was found that there are few studies that analyze the modifications

of short-circuit levels in microgrids due to the presence of EVs. Furthermore, none of them approach the problem from the point of view of the protection coordination. To fill this knowledge gap, this paper proposes to carry out a detailed study of short-circuit level modifications in microgrids due to the presence of EVs. In this case, the information provided in [20] is used, where a detailed analysis of the contributions of EVs to fault currents is carried out. Furthermore, the recommendation proposed in [19] regarding the inclusion of distributed generation and higher penetration of EVs in the fault analysis is also performed. Therefore, the contributions of this paper are twofold: (i) it presents a detailed study of the modifications of short-circuit levels in microgrids due to the presence of EVs considering different scenarios and (ii) an evaluation of the impact of EVs on the protection coordination schemes in microgrids is carried out.

The rest of this document is organized as follows. Section 2 describes different types of electric vehicle and their characteristics. Section 3 describes the effect of EVs under a fault condition. Section 4 presents the principle of operation of overcurrent protections in microgrids. Section 5 describes the proposed methodology for assessing the impact of EVs in short-circuit levels of microgrids. Section 6 illustrates the test and results, and finally, Section 7 presents the conclusions of the study.

2. Electric Vehicle Characteristics

An EV is a vehicle that is propelled by electricity, e.g., electric trains, subways, electric cars, etc. These types of vehicles are widely used, with the exception of electric cars, which although not a new technology, have gained prominence in recent years. This momentum is driven by the growing concern about climate change, which has generated a trend toward decarbonization and clean technologies. As a substitute for the internal combustion engine vehicle (ICEV), EVs powered by renewable electricity can reduce petroleum use and greenhouse gas emissions [24].

2.1. Types of Electric Vehicles

In today's electric vehicle market, there are different options to choose from: hybrid electric vehicle (HEV), plug-in hybrid electric vehicle (PHEV), battery electric vehicle (BEV) and fuel cell electric vehicle (FCEV). The main features of an EV are presented in Figure 1. The main characteristics, advantages and disadvantage of each type of EV are discussed in [4,25].

A HEV is similar to an ICEV but with an electric motor and a larger battery. The battery can be charged by regenerative braking and by the ICE at light loads. Typically, the battery and electric motor drive the vehicle at low speeds and the ICE drives the vehicle at high speeds. The electric motor can assist the ICE at high loads, improving vehicle performance and efficiency. HEVs present lower emissions and fuel consumption than ICEVs. These vehicles are not charged from the distribution network; therefore, they do not have any impact on the electric power system and also they cannot provide electric services to the grid.

A PHEV is an HEV with a battery that can be charged by regenerative braking by the ICE and also by connecting it to the grid. To extend the electric autonomy, it is characterized by higher electric motor power, a small ICE and higher battery capacity compared to an HEV. It can operate in all-electric mode and use only the electric motor, resulting in zero emissions. This type of EV generates few impacts on the power distribution system; nonetheless, its ability to provide electric services is limited.

A BEV has an electric motor powered by a battery and does not have an ICE. The electric autonomy depends on the capacity of the battery. The main advantage of this type of EV is that it does not produce emissions locally, which is very important in large cities. The battery is charged from the distribution network using different types of chargers, which generates different impacts on the power grid. In addition, during deceleration and braking, the motor works as a generator and produces electrical energy that charges the battery. It also allows electrical energy to flow from the battery to the AC motor in driving mode and from the AC motor to the battery in braking mode. The main challenge for BEVs

is the long charging period and limited public charging infrastructure. BEVs are expected to dominate the EVs market with future advances in battery technology and price reduction.

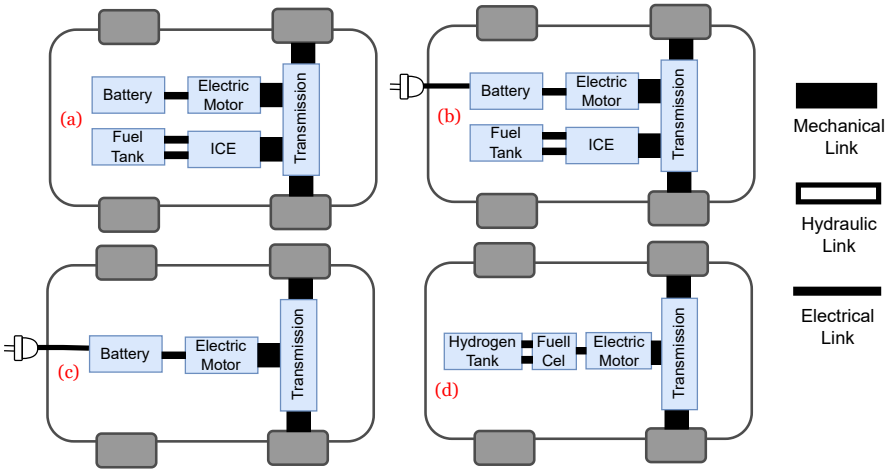


Figure 1. Basic structure of different electric vehicles (EVs) types. (**a**) Hybrid electric vehicle (HEV); (**b**) plug-in hybrid electric vehicle (PHEV); (**c**) battery electric vehicle (BEV); and (**d**) fuel cell electric vehicle (FCEV).

A FCEV runs on an electric motor like BEVs, but uses a fuel cell instead of a battery. These vehicles are recharged with hydrogen, and the fuel cell converts the chemical energy of the hydrogen gas into electrical energy that powers the EV engine. Hydrogen can be produced from fossil fuels, such as natural gas or water electrolysis. FCEVs have a short refueling time like ICEVs.

2.2. Plug-In Hybrid Electric Vehicle (PHEV) and Battery Electric Vehicle (BEV) Charging Methods

The availability of charging infrastructure is the most important factor driving EV adoption. According to [15,26,27], the EV charging infrastructure can be classified into three levels, according to the charging power rate, voltage, current and facility location. These levels identify the charging duration of EVs. Levels 1 and 2 have a slow charging characteristic, while level 3 has a fast charging one. The main features of the different charge levels of EVs are presented in Table 1. The charging infrastructure may have single-phase and three-phase chargers. The charging systems may be inside or outside the vehicle (see Figure 2), and there can be unidirectional or bidirectional chargers. Unidirectional charging has simple charging hardware and allows power to flow only from the grid to the EV. Bi-directional charging allows power to flow from the grid to the EV and can inject power from the EV battery to the grid (V2G), building (V2B) or home (V2H) [4]. Typically, the charging infrastructure consists of an AC/DC converter, power factor correction elements and a DC/DC converter.

Table 1. Charging level of EVs according to Refs. [1,4,15,24,25].

Charging Levels	Level 1	Level 2	Level 3
Phase	1 phase AC	1/3 phase AC	3 phase AC or DC
Voltage	120 V	240 V	208 V–600 V
Current	11 A, 16 A	16 A, 32 A, 80 A	240 A, 480 A
Power	1.4 kW, 1.9 kW	4 kW, 8 kW, 19.2 kW	50 kW, 100 kW
Installation	Domestic location	Domestic/Public location	Public location

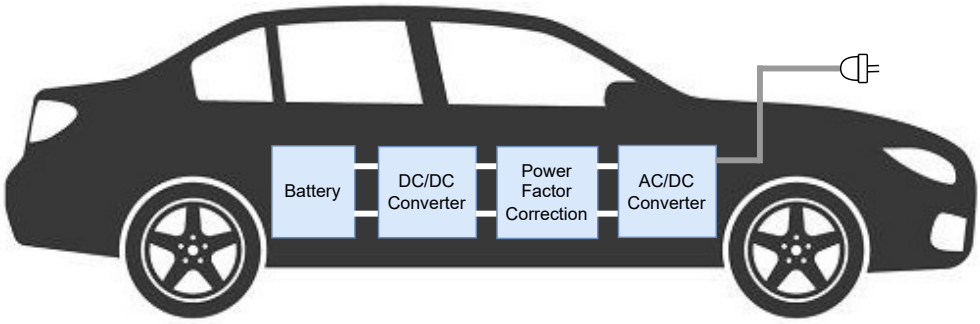


Figure 2. Structure of a slow charger station.

Charging level 1 represents a slow and simple way of charging, in this case, no additional infrastructure is needed and any wall outlet can be used. In countries with an operating frequency of 60 Hz, a standard 120 V wall outlet at 15 A is generally used. It is available only as an integrated charger and its cost is lower than other charging levels. Its main difficulty is that the EV needs a long time to fully charge. Due to its low power rating, this charging level has the lowest impacts on distribution systems.

Charging level 2 for 60 Hz operating frequency countries generally uses 208 V or 240 V outlets with currents up to 80 A and a charging power of 19.2 kW. Charging level 2, compared to level 1, has a shorter charging time. The difficulty with this charging level is that it requires dedicated electric vehicle supply equipment (EVSE) installation for public or home charging.

Charging level 3 is for fast charging and works as a commercial service station, as the vehicle charging time is less than 1 h. The charging station is similar to a conventional service station and can be built on the main roads and highways of cities. It is powered by a three-phase circuit with 480 V or higher voltages. It is available only as an external charger because the charging power is high and may exceed 100 kW. Level 3 charging is not suitable for home applications since it features a high installation cost, which represents a potential problem. The high charging power represents an advantage from the point of view of charging time, but it can generate large impacts on the power distribution grid.

3. Effects of EVs under a Fault Condition

EVs can impact the safety and reliability of electric systems, as well as increasing operating costs. The connection of EVs implies a considerable increase in electric system loads, which give rise to operating difficulties at peak hours stressing the energy market. From an operational point of view, EVs may lead to voltage stability problems, increase short-circuit levels and affect the power quality of the system [28].

Faults are a common phenomenon in distribution systems and microgrids, and have been studied in detail [29,30]. Nonetheless, it is important to highlight that the incorporation of PHEV- and BEV-type EVs generate impacts on short-circuit levels to be considered in electrical systems. Studies related to the modifications of short-circuit levels due to EVs are limited and few. Different types of chargers (unidirectional and bidirectional) depending on the number of vehicles incorporated in the network can produce considerable changes in fault characteristics [18,31]. V2G type charging stations generate a greater impact on the distribution grid due to their bidirectional functioning. Such chargers allow energy to flow from the grid to the EV and vice versa, which can impact short circuit levels on the grid.

The study of fault levels in distribution networks and microgrids considering the proliferation of EVs has not been widely analyzed in the specialized literature. For this reason, this article proposes to develop a detailed study of the modifications of the short-circuit levels in a benchmark microgrid. To carry out this study, the contributions presented in [20] are considered. This paper performs a detailed analysis of the contributions of EVs to fault currents, based on international standards [21–23], considering the actions of the battery energy storage systems (BESS) controllers and the characteristics of the interface power electronic converters (PECs). In [20], the authors propose a procedure to perform

the calculation of short-circuit currents considering the effect of BESS that are connected to the general grid by means of PECs. Therefore, to evaluate the modifications of the short-circuit levels in the analyzed test microgrid, the recommendations and procedures proposed in [20] are considered.

EVs charging systems have a direct current (DC) stage and an alternating current (AC) stage. Generally, the charging infrastructure consists of an AC/DC converter, power factor correction elements and a DC/DC converter as can be seen in Figures 2 and 3. Additionally, fast-charging stations are connected to the medium voltage grid by means of a transformer as shown in Figure 3. Fast charging stations have a greater impact on the grid and therefore generate great variations in short-circuit levels. For the above reasons, this paper concentrates on measuring the impact of fast-charging stations.

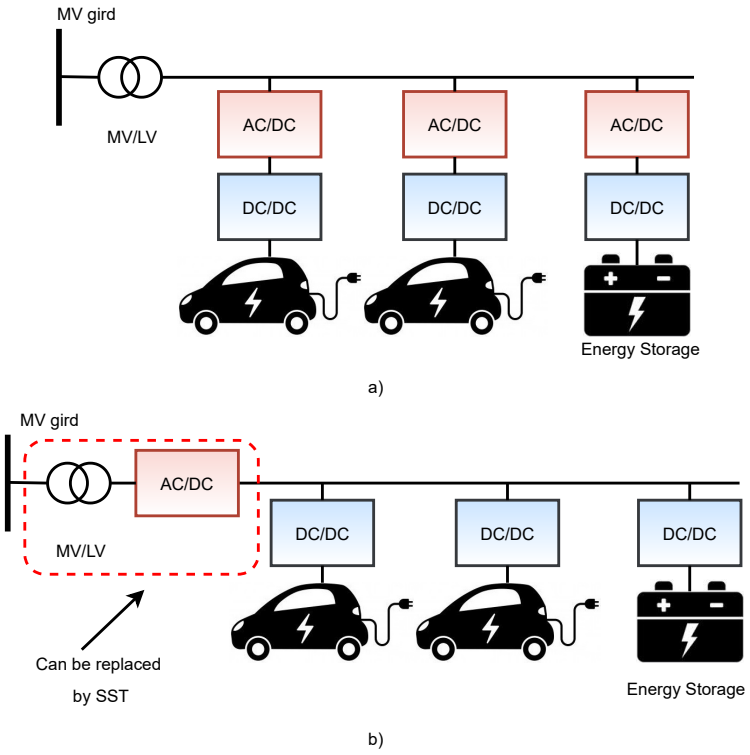


Figure 3. Structure of a fast-charger station: (**a**) with AC distribution network (**b**) with DC distribution network.

The EV charging infrastructure may experience several types of failures that can occur at different stages as shown in Figure 4. Note that it is possible to have F1-, F2- and F3-type faults. Fault F1 occurs in the DC stage, fault F2 takes place in the AC stage and fault F3 occurs in the network. For the purpose of this study, only F3-type faults are considered in order to observe the effect of the EVs on the short-circuit levels of the network.

According to [20], the fault current in a BESS can be determined as a combination of contributions from the batteries and the interface PECs. For a fault on the grid side (fault F3 in Figure 4), the contributions from the batteries and the PECs are set to a value greater than the rated current of the PECs. The final fault current in F3 is the sum of the BESS, PECs, and the grid contributions. The last ones would depend on specific characteristics of each grid.

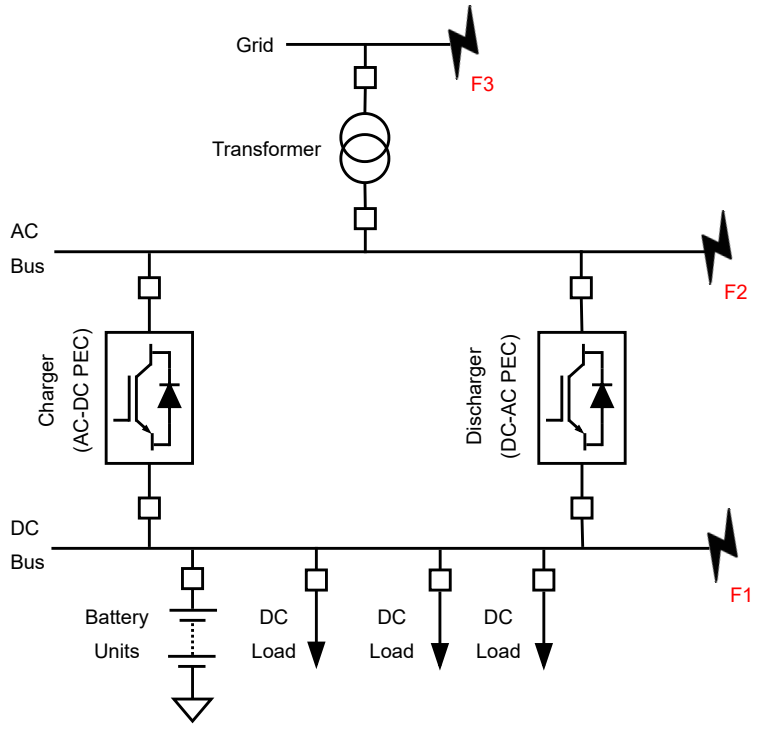


Figure 4. Type of faults in EVs fast-charge system.

4. Overcurrent Protections

Overcurrent protections are widely used in distribution systems and microgrids [32–34]. The incorporation of PHEV- and BEV-type EVs brings important modifications in short-circuit levels. As mentioned above, depending on the number of EVs incorporated in the network, different types of chargers (unidirectional and bidirectional) can produce considerable changes in fault characteristics [18,31]. Changes in short-circuit levels directly impact the performance of protection schemes. Therefore, V2G-type charging stations generate a greater impact on protection coordination schemes. This can lead to EVs impacting the safety and reliability of protection coordination schemes. To the best of the authors' knowledge, there are no studies in the specialized literature that approach in detail the impact of EVs on the protection schemes of distribution networks and microgrids. For this reason, in addition to the detailed study of the modifications of the short-circuit levels, this paper presents a detailed evaluation of the impact of EVs on the protection coordination schemes. Such analysis considers the recommendations presented in [20] regarding the the calculation of short circuits.

Protection coordination schemes in distribution networks and microgrids generally consist of overcurrent protections (OCPs) of different types. Among the most prominent OCPs are thermomagnetic circuit breakers (CBs), fuses, reclosers, overcurrent relays (OCRs) and directional overcurrent relays (DOCRs). OCRs include electromechanical relays (EMR) and static relays (SR). The main objective of an OCP scheme is to minimize the operating time by ensuring coordination between the main and backup OCPs. This is represented by Equation (1) where m and n are the number of relays and faults in the system, respectively, while t_{if} corresponds to the operating time of the OCP i when fault f occurs.

$$Min \sum_{i=1}^{m} \sum_{f=1}^{n} t_{if} \quad (1)$$

When a fault takes place, both backup and primary OCPs identify the occurrence of the fault. The backup OCP is in charge of tripping the fault in case the primary OCP fails to isolate it. Equation (2) illustrates this condition. In this case, t_{jf} is the operating time of the backup OCP j when fault f occurs, and t_{if} is the operating time of the primary OCP i when fault f occurs. The coordination time interval CTI is the period of time allowed for the backup protection to operate. This time is determined by the types of OCPs used. Typical CTI values are within the range of 0.2 to 0.5 s. The recommended minimum CTI are proposed in reference [35] and are presented in Table 2. For the coordination between fuses and CBs, the standard recommends clear space (CS) between curves.

$$t_{jf} - t_{if} \geq CTI \tag{2}$$

Table 2. Minimum CTIs [35].

Downstream	Fuse Upstream	CBs Upstream	EMR Upstream	SR Upstream
Fuse	CS	CS	0.22 s	0.12 s
CBs	CS	CS	0.22 s	0.12 s
EMR	0.2 s	0.20 s	0.30 s	0.20 s
SR	0.2 s	0.20 s	0.30 s	0.20 s

OCPs present a characteristic operating curve with which the operating time of the device is determined from the fault current flowing through it. The characteristic curves of CBs and fuses are varied and should generally consult each manufacturer. In the case of OCRs and DOCRs, the curves are standardized and governed by a specific function. Equation (3) describes a normally inverse characteristic curve. In this case, A and B are constant parameters of the curve, TMS_i is the time multiplier setting of relay i, and PSM_{if} is the ratio between the fault current I_{fi} and the pickup current $ipickup_i$ given by Equation (4).

$$t_{if} = \frac{A \cdot TMS_i}{PSM_{if}^B - 1} \tag{3}$$

$$PSM_{if} = \frac{I_{fi}}{ipickup_i} \tag{4}$$

Equation (5) indicates the operating time limits of the OCPs. In this case, t_{imin} and t_{imax} are the minimum and maximum operating times of OCP i, respectively.

$$t_{imin} \leq t_{if} \leq t_{imax} \tag{5}$$

Equation (6) represents the minimum and maximum limits of TSM for relay i given by TMS_{imin} and TMS_{imax}, respectively. Similarly, Equation (7) represents the lower and upper limits of the pickup current $ipickup_i$, denoted as $ipickup_{imin}$ and $ipickup_{imax}$, respectively.

$$TMS_{imin} \leq TMS_i \leq TMS_{imax} \tag{6}$$

$$ipickup_{imin} \leq ipickup_i \leq ipickup_{imax} \tag{7}$$

All protection schemes must meet the design and performance criteria, which are defined in detail in [36]. The first criterion that a protection scheme must meet is reliability. For this, it must operate correctly in the fault zone and it must guarantee the non-operation in faults outside the protection zone. The second criterion is sensitivity, i.e., it must detect any fault regardless of the degree of severity. The third criterion is speed, which translates into isolating the faulted zone as quickly as possible. The fourth criterion is selectivity, i.e., it must guarantee the maximum continuity of service with minimum disconnection of equipment from the system. Finally, the last criterion is simplicity.

Different indexes have been proposed in the literature to evaluate these criteria [37–39]. Some of these indices are used in this study to evaluate the performance of OCPs with EVs. The indices used in this study are described below.

The protection speed index (PSI) is a normalized index that indicates the variations in the operating speed of the protections in the event of changes in the scenarios analyzed. It is used in [39] and is shown in Equation (8). The numerator is the sum of the operating times of the primary and backup equipment after EVs installation and the denominator is the sum of the operating times of the primary and backup equipment for the original network. If the index is equal to zero, it means that there is no change in the system that affects the protections. If the index is greater than zero, it represents an improvement in the system in terms of operating times, so no change in the settings of the protections is required. Finally, if the index is negative, it means that the operating times are increased, which may require a change in the protection settings.

$$PSI = 1 - \frac{(\sum_{i=1}^{m} \sum_{f=1}^{n} t_{if})_{withEV}}{(\sum_{i=1}^{m} \sum_{f=1}^{n} t_{if})_{withoutEV}} \tag{8}$$

The operation time index (OTI) of the main protection equipment indicates the operating speed variation of each protection individually. It is the ratio between the operating time of the main protection considering EVs and the operating time of the same without EVs. This index is proposed in [37] and is presented in Equation (9). An OTI of 1 indicates that no change is presented, so no adjustments should be made. A value less than 1 indicates an improvement in the protection performance, so no settings should be changed. A value greater than 1 indicates a reduction in protection performance, and therefore, the protection settings must be adjusted.

$$OTI = \frac{t_{if-withEV}}{t_{if-withoutEV}} \tag{9}$$

The protection coordination index (PCI), given in MVA/s, is defined as the ratio of the rate of change of power to the rate of change of the CTI with EVs. A positive value indicates that an increase in the EVs penetration will result in a reduction in CTI. Higher PCI values at certain locations indicate that higher EVs penetration levels can be achieved with less impact on protection coordination (or in other words, with small changes in CTI). The PCI is proposed in [38] and is given by Equation (10).

$$PCI = \frac{\Delta P}{\Delta CTI} \tag{10}$$

5. Methodology

The main objective of this paper is to evaluate the impact of the incorporation of EVs on the performance of the existing protection coordination scheme of a microgrid. Initially, the electrical elements of the network are modeled in the DigSILENT PowerFactory software, and the operating scenarios to be considered are adjusted. Lines, generators, transformers, loads, protections and charging stations are characterized in the model. In the adjustment of the each scenarios, the generation dispatch and number of vehicles to be considered are defined.

Once the network modeling is completed, a study of the short-circuit levels in the main buses of the network is carried out. Short-circuit calculations are performed for each scenario. In this case, the scenarios without EVs are defined as base cases, and the variation of the short-circuits with the incorporation of EVs is analyzed. According to the variations of the short-circuit levels, an initial analysis can be performed to identify scenarios that may present negative variations in the coordination scheme.

According to the information obtained in the short-circuit study, the impact of EVs in the protection scheme is evaluated. For this purpose, several short circuits are performed on the lines of the network, and the currents seen by the protections of each element are obtained. Once the short-circuit values for each scenario are obtained, the results are evaluated using the equations presented in Section 4. The results are analyzed, and the impact on the existing scheme is measured. Finally, once the performance of the protection scheme is evaluated with the incorporation of EVs, some of the cases analyzed are verified by means of the coordination curves.

6. Tests and Results

A benchmark IEC microgrid integrating different types of DG technologies was used to test the proposed approach. The parameters of the microgrid, depicted in Figure 5, can be found in [40]. The IEC microgrid is a distribution network that integrates different DG sources as presented in Figure 5. The grid operates at 24 kV and it features 4 DG sources with their respective step-up transformers; it also has 5 distribution lines, 11 buses and 6 loads. This test system is widely known and has been used in several protection coordination studies [41–43].

A base case (BC) and five different scenarios changing the presence of DG and EVs were considered (see Table 3). In this case, the BC scenario does not take into account DG and represents a traditional radial distribution network. In the BC scenario, the load is fed through the main grid. In scenario EV1, the DG units are still disconnected; nonetheless, there are 6 EVs connected to the grid. In scenario EV2, the DG units remain disconnected, but there are 18 EVs in the network. The second base case scenario is denoted as BC DG. In this case, the DG units are connected to the grid; therefore, the load is fed by the DG units and the main grid. In scenario EV1 DG, the DG units are connected to the grid, and there are also 6 EVs. Finally, in scenario EV2 DG, the DG units are connected to the grid, and there are 18 EVs. In the tests carried out, 6 electric vehicle charging stations (EVCS) were incorporated and distributed as illustrated in Figure 5. In all cases, 100 kW level 3 battery chargers were considered.

Table 3. Scenarios under analysis.

Scenario	DG	EVCS 1	EVCS 2	EVCS 3	EVCS 4	EVCS 5	EVCS 6	Total EVs
BC	OFF	0 EVs	0 EVs	0 EVs	0 EVs	0 EVs	0 EVs	0 EVs
EV1	OFF	1 EVs	1 EVs	1 EVs	1 EVs	1 EVs	1 EVs	6 EVs
EV2	OFF	3 EVs	3 EVs	3 EVs	3 EVs	3 EVs	3 EVs	18 EVs
BC DG	ON	0 EVs	0 EVs	0 EVs	0 EVs	0 EVs	0 EVs	0 EVs
EV1 DG	ON	1 EVs	1 EVs	1 EVs	1 EVs	1 EVs	1 EVs	6 EVs
EV2 DG	ON	3 EVs	3 EVs	3 EVs	3 EVs	3 EVs	3 EVs	18 EVs

Regarding the protection coordination scheme, the network is protected with 15 DOCRs, which are labeled with numbers ranging from 1 to 15 preceded by the letter R as indicated in Figure 5. The settings and characteristics of the DOCRs used in this study are presented in Table 4 and were taken from [44]. Table 4 indicates the transformation ratio of the current transformers RCT, as well as the pickup current i_{pickup} and dial TMS of each relay. Regarding the dial, one setting is considered for the scenarios without DG and another one for the scenarios with DG. The test system was implemented and simulated in DigSILENT PowerFactory. To evaluate the protection scheme, five three-phase faults at lines DL-1, DL-2, DL-3, DL-4, and DL-5 were considered. Calculations and tests were performed according to the recommendations of the IEEE Standard 242, which is widely used for overcurrent protection coordination. This paper considers a CTI of 0.3 s for comparative purposes. For the operation time of the DOCRs, the IEC normal inverse curve with constants A and B of 0.14 and 0.02, respectively, was considered.

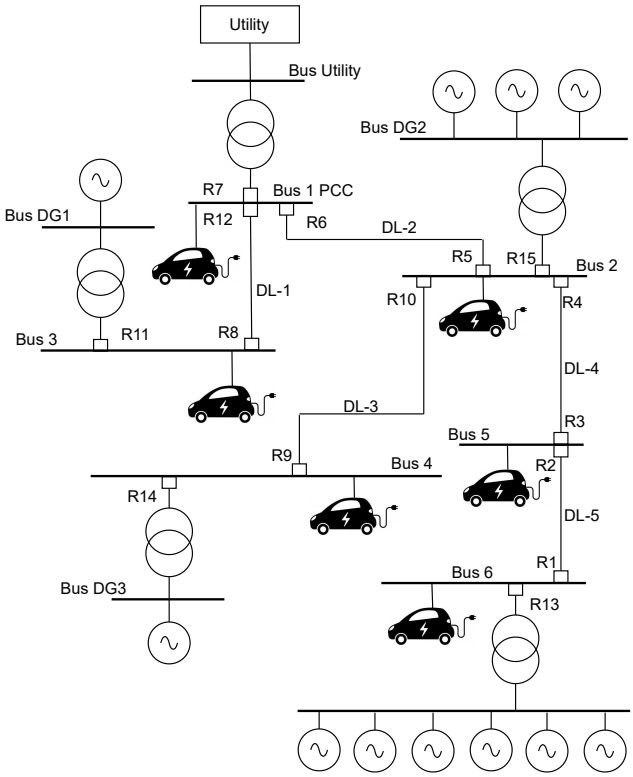


Figure 5. Benchmark IEC microgrid with EVs.

Table 4. *RCT* and i_{pickup} for each relay.

Relay	*RCT*	i_{pickup}	*TMS* without DG	*TMS* with DG
R1	400	0.50		0.1370
R2	400	0.50	0.05	0.050
R3	400	0.50		0.050
R4	400	0.50	0.1787	0.1891
R5	400	0.50		0.1148
R6	400	0.50	0.3223	0.3198
R7	1200	1.00	0.2060	0.2439
R8	400	0.50		0.1911
R9	400	0.50		0.050
R10	400	0.50	0.050	0.050
R11	400	0.65		0.2175
R12	400	0.50	0.050	0.050
R13	400	0.88		0.1669
R14	400	0.65		0.0998
R15	400	0.55		0.1359

The results section is divided in two subsections. Initially, short-circuit levels are evaluated at each bus of the test system and their variations are compared considering the scenarios described in Table 3. Then, the coordination of the protection scheme is evaluated using the settings and characteristics proposed in [44] by means of the constraints and indexes indicated in Section 5. To this end, a fault in the protected element is performed to compare the operating times of the main relays with the backup relays.

6.1. Modifications in Short-Circuit Currents

To evaluate the impact of the incorporation of EVs in the proposed network, an analysis of the short-circuit levels considering the main buses of the network was carried out. Faults in all buses were performed for each of the scenarios presented in Table 3. The results are presented in Figure 6. It can be seen that the incorporation of EVs increases the short-circuit levels. In scenarios EV1 and EV2, where DG is disconnected, there is an increase in short-circuit levels at all buses compared to the base case (BC). Note that of

this group of scenarios, EV2 presents the highest short-circuit levels. When considering DG connected to the grid (scenarios EV1 DG and EV2 DG), there is also an increase in short-circuit levels at all buses compared to the corresponding base case with DG (scenario BC DG). Note that scenario EV2 DG presents the highest short-circuit levels. Note that the highest increments in short-circuit levels take place when DG is connected to the network. Finally, it was observed that Bus 1 PCC features the highest magnitudes of short-circuit, which is due to its proximity to the main grid.

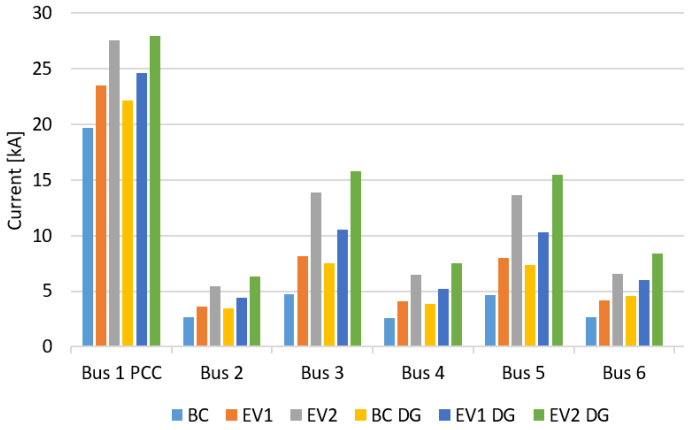


Figure 6. Short-circuit levels in all scenarios.

The percentage change in short-circuit levels was measured in order to have a numerical reference of the modifications. For this purpose, the short-circuit levels of BC and BC DG scenarios were defined as the base data. The percentages presented in Figures 7 and 8 indicate the increment in short-circuit levels of the scenarios that consider the incorporation of EVs with respect to the base case. Figure 7 shows the results of the scenarios without DG, while Figure 7 presents the results of the scenarios that consider DG in the network. Note that in none of the analyzed scenarios, the short-circuit levels are reduced; in all cases, they increase with respect to the base case.

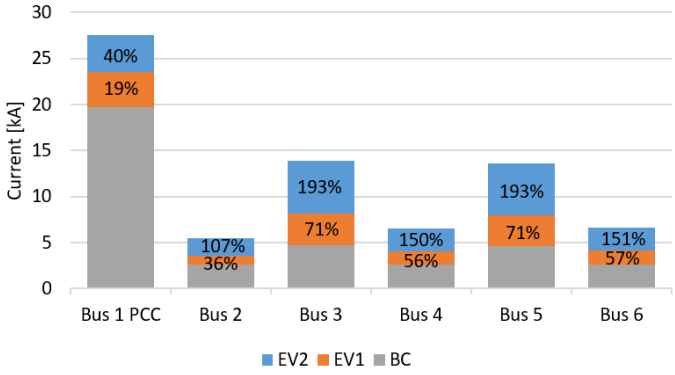


Figure 7. Short-circuit scenarios without DG.

From Figure 7, it can be seen that EVs impose a considerable increase in short-circuit levels when there is no DG connected to the network. Scenario EV1, which considers 5 EVs, presents a smaller increase in short-circuit levels compared to scenario EV2, which considers 15 EVs. Note that Bus 1 PCC presents the lowest short-circuit percentage increase in both scenarios: 19% in EV1 and 40 % in EV2. This is due to the high short-circuit level of the bus, which is related to its proximity to the main grid. Buses 3 and 5 present the highest short-circuit percentage increase: 71% for scenario EV1 and 193 % scenario EV2. According to these results, it can be inferred that the most affected protections are those at Buses 3 and 5, due to their large short-circuit level variations.

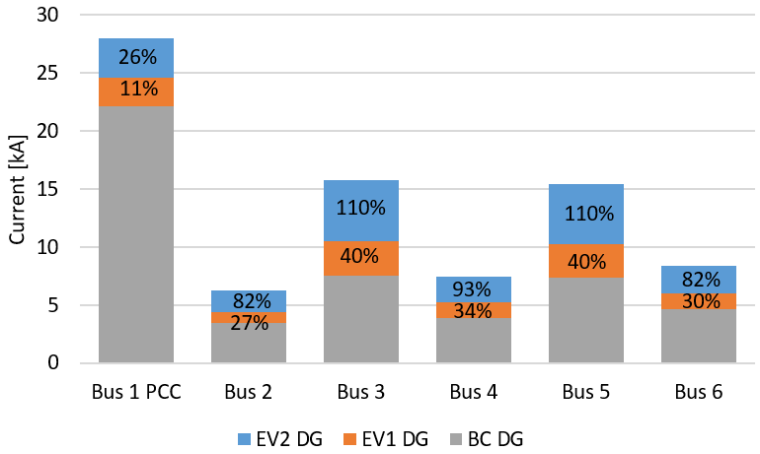


Figure 8. Short-circuit scenarios with DG.

From Figure 8, it can be seen that there is also an increment in the short-circuit levels when DG is connected to the network; nonetheless, such an increment is lower than that of the previous case illustrated in Figure 7. In scenario EV1 DG, which considers 5 EVs, there is a smaller increase compared to scenario EV2 DG that considers 15 EVs. As in the previous case (without DG), Bus 1 PCC has the lowest percentage increase in short-circuit levels: 11% in scenario EV1 GD and 26% in scenario EV2 DG. Furthermore, Buses 3 and 5 present the highest increment in short-circuit levels: 40% and 110% in scenarios EV1 DG and EV2 DG, respectively. According to these results, it can be seen that the protections that may have the greatest impact are those at Buses 3 and 5 due to their large short-circuit level variations.

Comparing the results of the scenarios with and without GD, it can be concluded that the latter presents the greatest variations in short-circuit levels when incorporating EVs. This suggests that there will be a greater impact on the protection schemes in those systems that have their DG units disconnected from the main grid.

6.2. Effects on the Protection Coordination Scheme

After the assessment of the short-circuit levels developed in the previous section, the evaluation of the protection coordination scheme is carried out. In order to evaluate the existing DOCR scheme in the network, and for comparative purposes, five three-phase faults are considered in lines DL-1, DL-2, DL-3, DL-4 and DL-5. Once the faults are executed, the performance of the existing scheme is evaluated using the equations, constraints and indexes presented in Section 4. Initially, the performance of the scheme is globally evaluated, using Equations (1), (2), (8) and (10); subsequently, the performance of the scheme is particularly evaluated, measuring the performance of each protection, using Equations (2) and (9). Finally, the results obtained from the evaluations performed with the equations, constraints and indexes presented in Section 4 are contrasted against the analysis of the traditional coordination curves.

The results to generally evaluate the DOCR protection scheme of the network are presented in Tables 5–7. Tables 5 and 6 present the operation time T, given by Equation (1), and the number of violations V of Equation (2) for scenarios considering the DG, disconnected and connected, respectively. Table 7 presents the PSI and PCI indices for all scenarios.

Table 5. Operating time and coordination violations for scenarios without DG.

Scenarios	$T[seg]$	V
BC	4.99	0
EV1	11.65	2
EV2	7.48	3

Table 6. Operating time and coordination violations in scenarios with DG.

Scenarios	$T[seg]$	V
BC DG	13.66	0
EV1 DG	18.36	0
EV2 DG	18.62	2

Table 7. PSI and PCI indices.

Index	BC vs. EV1	BC vs. EV2	BC GD vs. EV1 DG	BC GD vs. EV2 DG
PSI	−1.33	−0.49	−0.34	−0.36
PCI	25.55	58.87	130.71	71.82

From Table 5, it can be observed that in the BC scenario, there are no coordination problems since the number of violations of Equation (2) is zero; furthermore, the total operating time of the protections is the shortest one. With the connection of 5 EVs (scenario EV1), there are coordination problems since two violations of Equation (2) appear and the operation time also increases to 11.65 s. With respect to scenario EV2, which considers 15 EVs, the coordination problems increase since there are three violations of Equation (2).

In Table 6, it can be seen that in the BC DG scenario, there are no coordination problems since there are no violations of Equation (2), and the total operating time of the protections is the shortest one. With scenario EV1, there are no coordination problems; nonetheless, the total operating time increases to 18.36 s. In scenario EV2 DG, there are coordination problems represented in two violations of Equation (2), and the operation time also increases.

Table 7 shows the PSI and PCI indices described in described in Section 4 for all scenarios. The negative sign of the PSI index indicates that there was a reduction in the operating speed of the DOCR scheme in all scenarios. This evidences that the increase in EVs in the network affects the performance of the DOCR scheme. From the PSI index, it can also be identified that the impact is greater in scenarios without DG.

According to the sign of the PCI index, there is a reduction in the CTI, which indicates that the protection coordination is affected. The PCI index shows that the increase in EVs in the network affects the performance of the DOCR scheme. It can also be concluded from the PCI index that the scenarios with DG show a lower impact on the protection coordination (smaller changes of the CTI) than those scenarios without DG.

After the evaluation of the general indexes of the DOCR scheme, the particular evaluation of each of the relays is carried out. The results of this evaluation are presented in Tables 8 and 9.

Table 8. OTI index.

Relay	BC vs. EV1	BC vs. EV2	BC GD vs. EV1 DG	BC GD vs. EV2 DG
R1			0.90	0.76
R2	0.94	0.86	0.98	0.91
R3			0.76	0.60
R4	0.93	0.84	0.98	0.91
R5			0.94	0.94
R6	1.02	1.00	1.04	1.03
R7				
R8			0.84	0.65
R9			0.61	0.54
R10	0.94	0.86	0.93	0.90
R11				
R12	1.02	1.01	1.07	1.06
R13				
R14				
R15				

Table 9. Coordination time interval (CTI) for all scenarios.

CTI	BC	EV1	EV2	BC DG	EV1 DG	EV2 DG
R3–R1	✓	✓	✓	✓	✓	✓
R4–R2	✓	✓	X	✓	✓	✓
R1–R3	✓	X	X	✓	✓	X
R6–R4	✓	✓	✓	✓	✓	✓
R15–R4	✓	✓	✓	✓	✓	X
R15–R5	✓	✓	✓	✓	✓	✓
R7–R6	✓	X	✓	✓	✓	✓
R8–R6	✓	✓	X	✓	✓	✓
R11–R8	✓	✓	✓	✓	✓	✓
R14–R9	✓	✓	✓	✓	✓	✓
R6–R10	✓	✓	✓	✓	✓	✓
R15–R10	✓	✓	✓	✓	✓	✓
R5–R12	✓	✓	✓	✓	✓	✓
R7–R12	✓	✓	✓	✓	✓	✓

Using the general indices, it can be concluded that the increase in EVs in the network has a negative impact on the protection coordination scheme. It can also be concluded that in scenarios with DG, the impact is slightly lower. This shows that the impact of EVs on protection coordination schemes can be higher in networks with low short-circuit levels. These analyses are in agreement with those initially performed on the short-circuit levels presented in Section 6.2.

After the evaluation of the general indexes, the particular evaluation of each relay of the protection coordination scheme is carried out. The results are presented in Tables 8 and 9. In Table 8, the OTI index is presented. This index allows to evaluate the operating speed of each relay. From the OTI index, it can be identified that in all scenarios, the operating speed of R6 and R12 are negatively impacted since the index has a value greater than 1; the other relays have a positive or very similar impact on the operating speed.

In Table 9, the selectivity of each one of the protections is evaluated in the applicable cases according to the recommendations and analysis proposed in [42–44]. Table 9 indicates the cases where selectivity is lost. Selectivity is evaluated using Equation (2). In the CTI column, the relay on the right is the main relay, and the relay on the left is the backup. From the selectivity results, it can be seen that in scenarios BC, BC DG and EV1 DG, there is no coordination problem. In scenario EV1, selectivity is lost in two cases: the first one when the main relay is R3 and the backup relay is R1; and the second one when the main relay is R6 and the backup relay is R7. In scenario EV2 DG, selectivity is lost in two cases: when the main relay is R3 and the backup is R1; and when the main relay is R4 and the backup is R15. In scenario EV2, selectivity is lost in three cases: when the main relay is R3 and the backup is R1; when the main relay is R2 and the secondary is R4; and when the main relay is R6 and the secondary is R8. From the selectivity analysis of each relay, it can also be concluded that the impact of EVs is lower in scenarios with DG connected to the network.

Once the selectivity is analyzed by verifying compliance with Equation (2), some of the cases are validated using the coordination curves. The first case to be analyzed is when there is a fault on line DL-4. In this case, relay R3 is the main relay and R1 is the backup relay. In the BC scenario, R3 does not see the fault current because the contributions to this current come from the main network; consequently, in this scenario, it is not necessary to verify the coordination of these relays. Therefore, when analyzing scenarios EV1 and EV2, there are selectivity problems. In scenario BC DG, it is necessary to coordinate relays R3 and R1 (see Figure 9) and there is no problem with selectivity. In scenario EV1 DG, there is also no problem with selectivity (see Figure 10), while in scenario EV2 DG, selectivity is lost (see Figure 11) because the CTI is lower than 0.3 s.

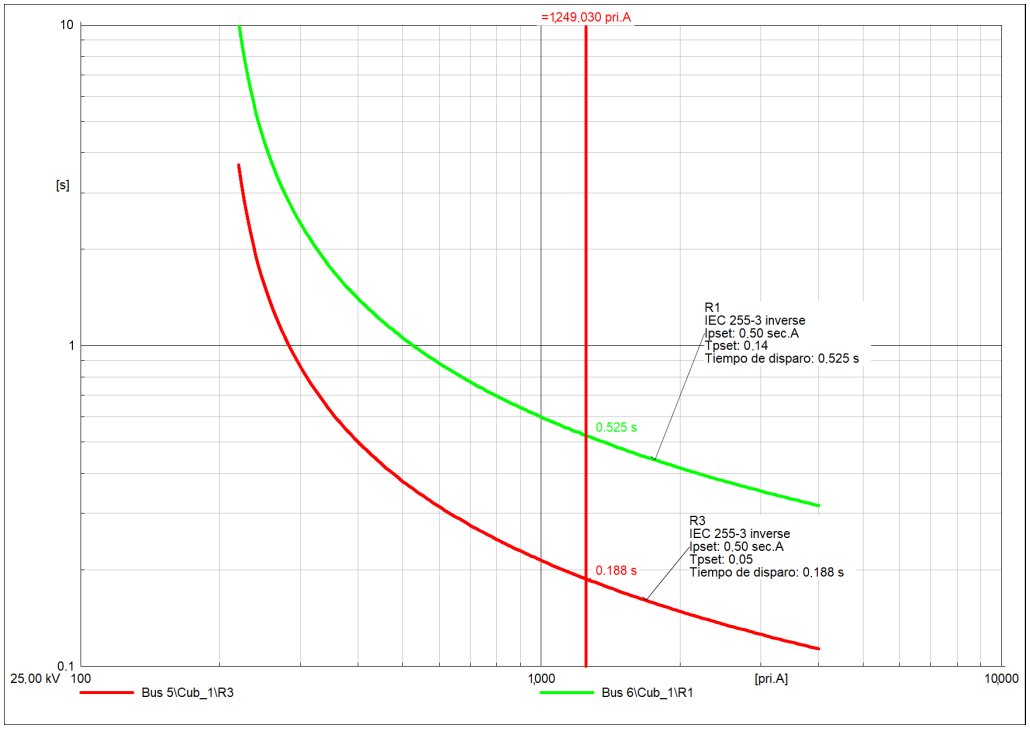


Figure 9. Coordination curve R1–R3 line fault DL-4 scenario BC DG.

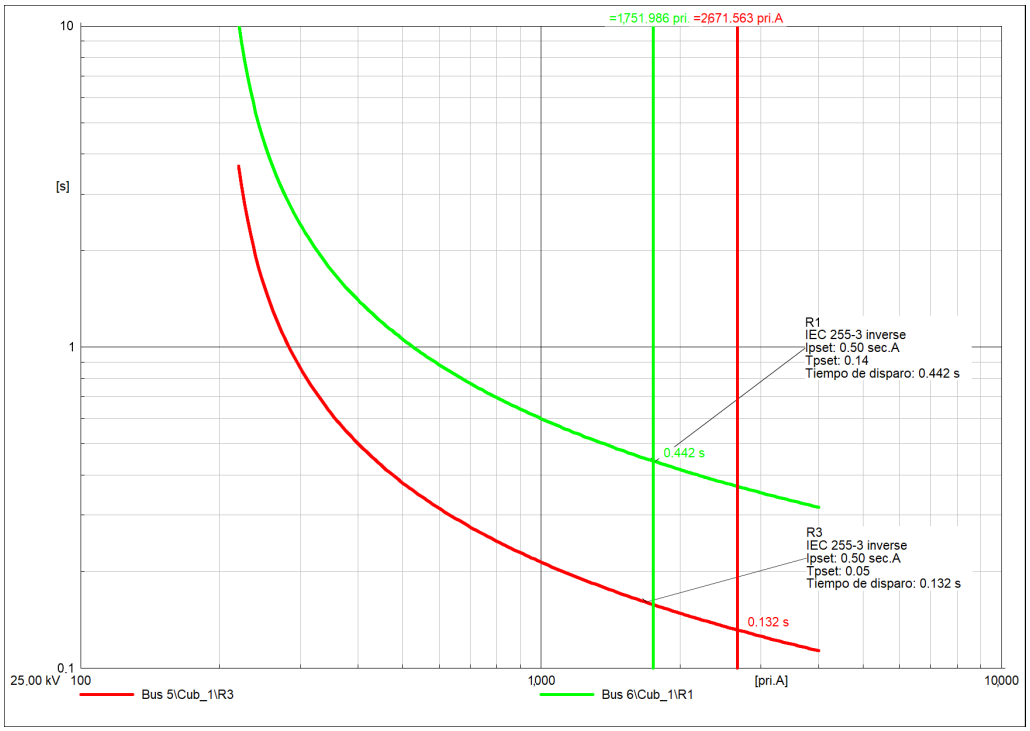


Figure 10. Coordination curve R1–R3 line fault DL-4 scenario EV1 DG.

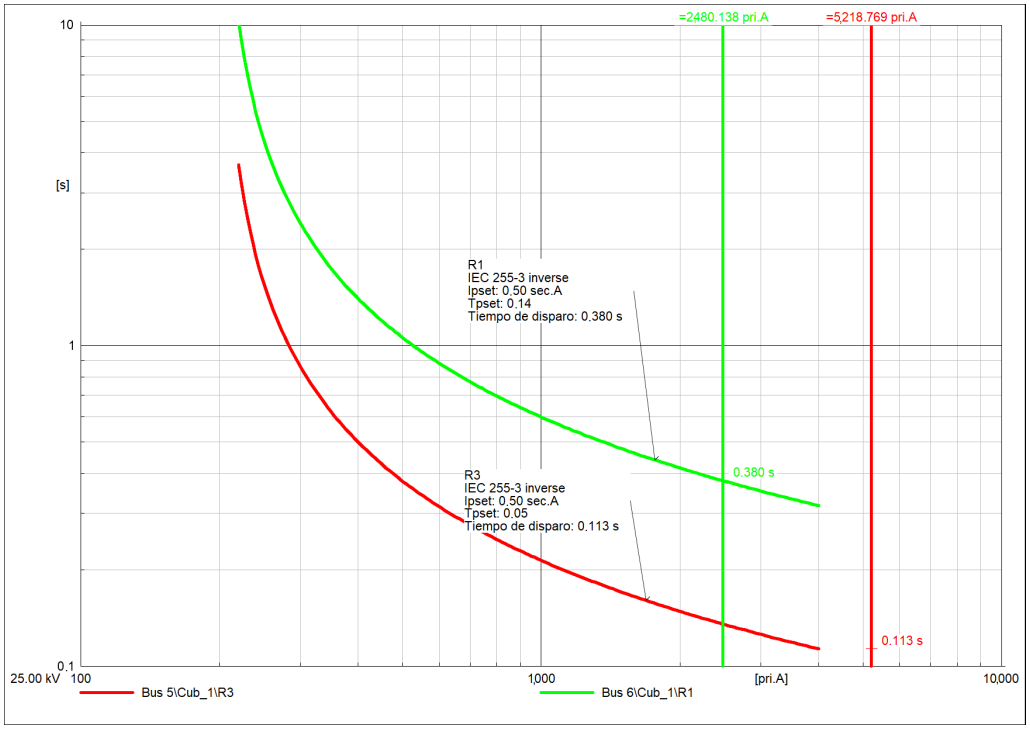


Figure 11. Coordination curve R1–R3 line fault DL-4 scenario EV2 DG.

The second case to be analyzed is when there is a fault on line DL-3. In this case, relay R6 is the main relay and R7 is the backup relay. In the BC scenario relays, R6 and R7 present selectivity as in the other scenarios (see Figure 12). In scenario EV1, selectivity is lost because the CTI is lower than 0.3 s (see Figure 13).

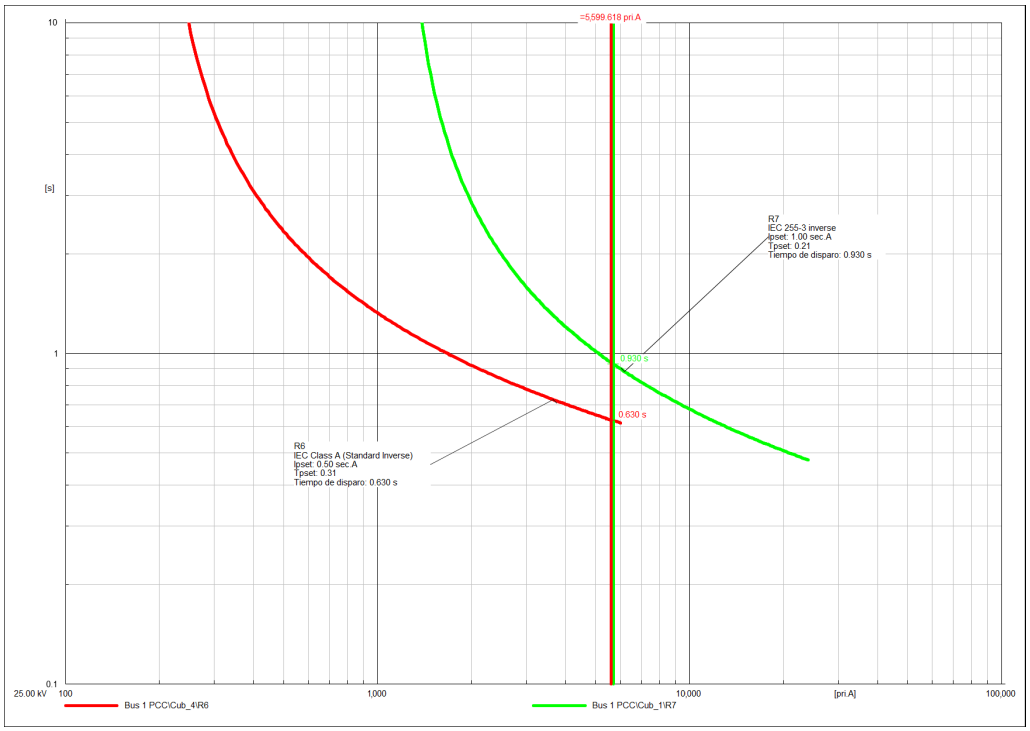


Figure 12. Coordination curve R7–R6 line fault DL-3 scenario BC.

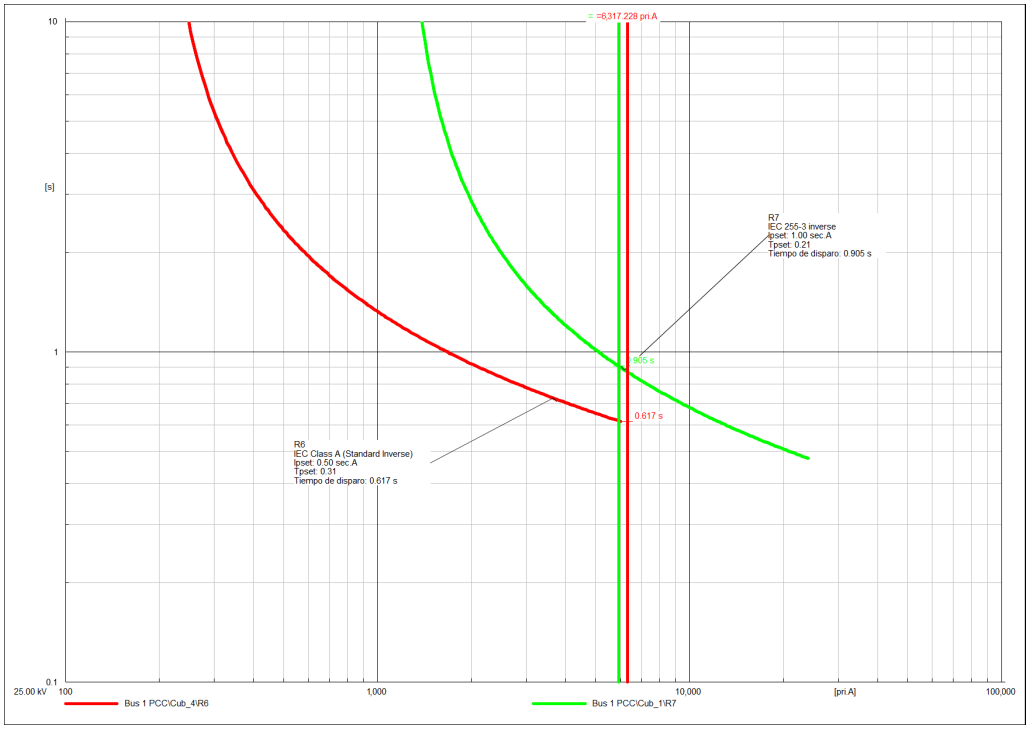


Figure 13. Coordination curve R7–R6 line fault DL-3 scenario EV1.

The third case to be analyzed is when there is a fault on line DL-5. In this case, relay R2 is the main relay, and R4 is the backup relay. In the BC scenario, relays R2 and R4 present selectivity (see Figure 14), as in the other scenarios; nonetheless, in scenario EV2, selectivity is lost (see Figure 15) because the CTI is lower than 0.3 s.

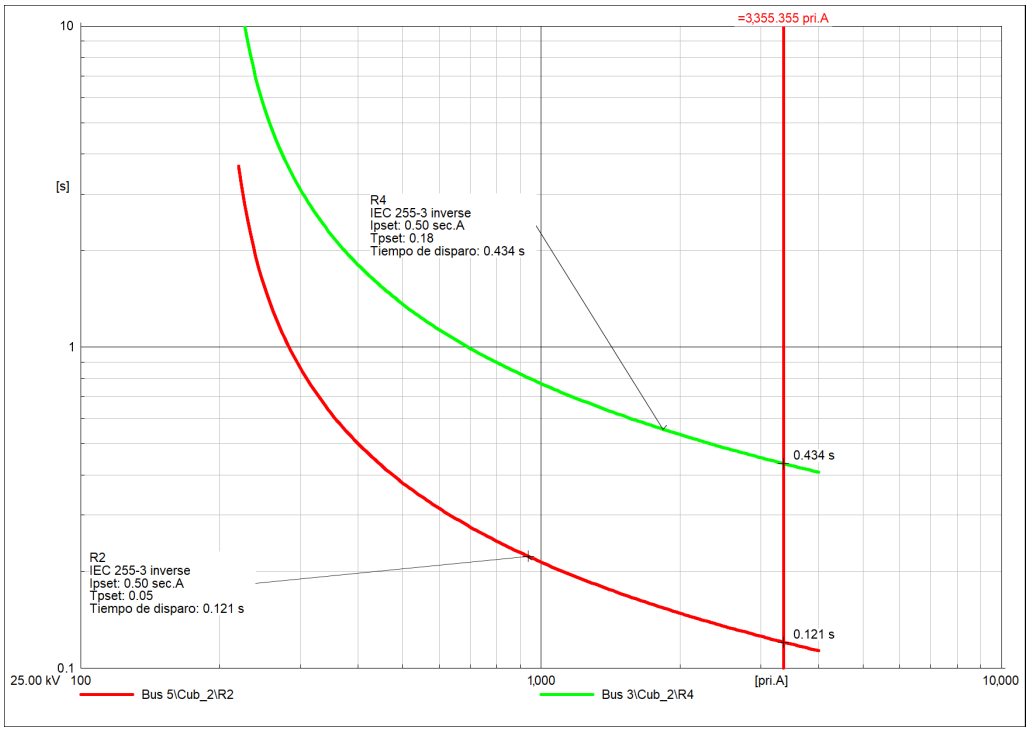


Figure 14. Coordination curve R4–R2 line fault DL-5 scenario BC.

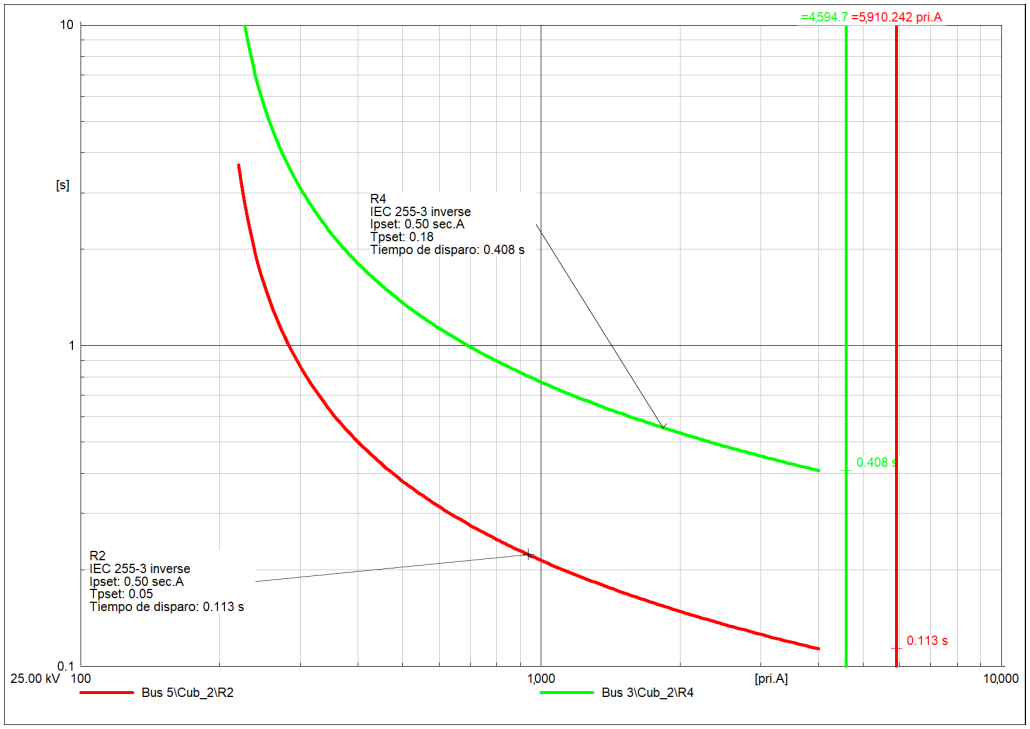


Figure 15. Coordination curve R4–R2 line fault DL-5 scenario EV2.

7. Conclusions

Given the complex nature of today's distribution grids, the increasing presence of renewable DG in microgrids and the growing incorporation of EVs, a detailed assessment of protection coordination schemes is needed. In a context in which microgrids are expected to incorporate a greater number of ultra-fast EVs chargers, studies are required to measure the impact of these elements on the grid. This paper evaluates the impact on short-circuit levels and protection coordination schemes in microgrids with the incorporation of EVs. According to the results obtained, it can be concluded that EVs impact the performance of protection coordination schemes in microgrids. This impact will depend on the number of EVs incorporated in the network and on the characteristics of the network itself. It is observed that as the number of EVs incorporated in the notwork increases, the impact on the coordination scheme becomes greater. It is also shown that the network characteristics define the level of impact; for example, in networks with low short-circuit levels, the effects of EVs on the protection schemes are greater. According to the results, it can be concluded that in microgrids with a high presence of DG, the impact of EVs may be slightly lower than in networks with a low presence of DG.

Author Contributions: Conceptualization, S.D.S.-Z. and J.M.L.-L.; Data curation, S.D.S.-Z.; Formal analysis, S.D.S.-Z., C.D.Z.R., A.V.J. and J.M.L.-L.; Funding acquisition, C.D.Z.R. and A.V.J.; Investigation, S.D.S.-Z., J.M.L.-L., C.D.Z.R. and A.V.J.; Methodology, S.D.S.-Z.; Project administration, S.D.S.-Z., A.V.J. and C.D.Z.R.; Resources, S.D.S.-Z., C.D.Z.R. and J.M.L.-L.; Software, S.D.S.-Z.; Supervision, C.D.Z.R. and J.M.L.-L.; Validation, S.D.S.-Z., C.D.Z.R. and J.M.L.-L.; Visualization, S.D.S.-Z., C.D.Z.R., A.V.J. and J.M.L.-L.; Writing—original draft, S.D.S.-Z.; Writing—review and editing, S.D.S.-Z., C.D.Z.R., A.V.J. and J.M.L.-L. All authors have read and agreed to the published version of the manuscript.

Funding: This study was funded by the Agencia de Educación Postsecundaria de Medellín-Sapiencia under the agreement 723 of 2021 and the project SM202013.

Institutional Review Board Statement: Not applicable.

Informed Consent Statement: Not applicable.

Data Availability Statement: Data is available via authors through email.

Acknowledgments: The authors gratefully acknowledge the support from the Agencia de Educación Postsecundaria de Medellín-Sapiencia under agreement 723 of 2021 and the project SM202013. The authors also want to acknowledge to the Institución Universitaria Pascual Bravo for its support through the project SM202013.

Conflicts of Interest: The authors declare no conflict of interest.

Abbreviations

This section presents the nomenclature and abbreviations used in the paper for quick reference.

t_{if}	Operating time of overcurrent protection i when fault f occurs
$ipickup$	Pickup current
m, n	Number of relays and faults, respectively
t_{imin}	Minimum operating time of overcurrent protection i
t_{imax}	Maximum operating time of overcurrent protection i
TMS_{imin}	Minimum limit of time multiplier setting i
TMS_{imax}	Maximum limit of time multiplier setting i
$ipickup_{imin}$	Minimum limit of pickup current i
$ipickup_{imax}$	Maximum limit of pickup current i
I_{fi}	Fault current of overcurrent protection i
BEV	Battery electric vehicle
$BESS$	Battery energy storage system
CTI	Coordination time interval
DG	Distributed generation
$DOCR$	Directional overcurrent relay
EV	Electric vehicle
$EVCS$	Electric vehicle charging station
$FCEV$	Fuel cell electric vehicle
HEV	Hybrid electric vehicle
$ICEV$	Internal combustion engine vehicle
OTI	Operation time index
PMS	Plug multiplier setting
PSI	Protection speed index
$PHEV$	Plug-in hybrid electric vehicle
PCI	Protection coordination index
$PECs$	Power electronic converters
TMS	Time multiplier setting
$V2B$	Vehicle to building
$V2G$	Vehicle to grid
$V2H$	Vehicle to home

References

1. Tu, H.; Feng, H.; Srdic, S.; Lukic, S. Extreme fast charging of electric vehicles: A technology overview. *IEEE Trans. Transp. Electrif.* **2019**, *5*, 861–878.
2. Tong, L.; Zhao, S.; Jiang, H.; Zhou, J.; Xu, B. Multi-Scenario and Multi-Objective Collaborative Optimization of Distribution Network Considering Electric Vehicles and Mobile Energy Storage Systems. *IEEE Access* **2021**, *9*, 55690–55697. [CrossRef]
3. Tabatabaei, J.; Moghaddam, M.S.; Baigi, J.M. Rearrangement of Electrical Distribution Networks With Optimal Coordination of Grid-Connected Hybrid Electric Vehicles and Wind Power Generation Sources. *IEEE Access* **2020**, *8*, 219513–219524. [CrossRef]
4. Nour, M.; Chaves-Ávila, J.P.; Magdy, G.; Sánchez-Miralles, Á. Review of positive and negative impacts of electric vehicles charging on electric power systems. *Energies* **2020**, *13*, 4675.
5. Amjad, M.; Farooq-i-Azam, M.; Ni, Q.; Dong, M.; Ansari, E.A. Wireless charging systems for electric vehicles. *Renew. Sustain. Energy Rev.* **2022**, *167*, 112730. [CrossRef]
6. Connor, W.D.; Wang, Y.; Malikopoulos, A.A.; Advani, S.G.; Prasad, A.K. Impact of Connectivity on Energy Consumption and Battery Life for Electric Vehicles. *IEEE Trans. Intell. Veh.* **2021**, *6*, 14–23. [CrossRef]
7. Pieltain Fernández, L.; Gomez San Roman, T.; Cossent, R.; Mateo Domingo, C.; Frías, P. Assessment of the Impact of Plug-in Electric Vehicles on Distribution Networks. *IEEE Trans. Power Syst.* **2011**, *26*, 206–213. [CrossRef]
8. Lopes, J.A.P.; Soares, F.J.; Almeida, P.M.R. Integration of electric vehicles in the electric power system. *Proc. IEEE* **2010**, *99*, 168–183.
9. Dharmakeerthi, C.; Mithulananthan, N.; Saha, T. Impact of electric vehicle fast charging on power system voltage stability. *Int. J. Electr. Power Energy Syst.* **2014**, *57*, 241–249.

10. Deb, S.; Tammi, K.; Kalita, K.; Mahanta, P. Impact of electric vehicle charging station load on distribution network. *Energies* **2018**, *11*, 178.
11. Suwanapingkarl, P.; Prakobkit, S.; Srivallop, K.; Boonthienthong, M. Reviews: The Impacts of Electric Vehicles (EVs) and Renewable Energy Resources (REs) on The Distribution Power Network. In Proceedings of the 2020 International Conference on Power, Energy and Innovations (ICPEI), Chiangmai, Thailand, 14–16 October 2020; pp. 93–96. [CrossRef]
12. Aghajan-Eshkevari, S.; Azad, S.; Nazari-Heris, M.; Ameli, M.T.; Asadi, S. Charging and discharging of electric vehicles in power systems: An updated and detailed review of methods, control structures, objectives, and optimization methodologies. *Sustainability* **2022**, *14*, 2137. [CrossRef]
13. Sadeghian, O.; Nazari-Heris, M.; Abapour, M.; Taheri, S.S.; Zare, K. Improving reliability of distribution networks using plug-in electric vehicles and demand response. *J. Mod. Power Syst. Clean Energy* **2019**, *7*, 1189–1199.
14. Dulău, L.I.; Bică, D. Effects of electric vehicles on power networks. *Procedia Manuf.* **2020**, *46*, 370–377.
15. Al-Hanahi, B.; Ahmad, I.; Habibi, D.; Masoum, M.A.S. Charging Infrastructure for Commercial Electric Vehicles: Challenges and Future Works. *IEEE Access* **2021**, *9*, 121476–121492. [CrossRef]
16. Turan, M.T.; Gökalp, E. Integration Analysis of Electric Vehicle Charging Station Equipped with Solar Power Plant to Distribution Network and Protection System Designs. *J. Electr. Eng. Technol.* **2022**, *17*, 903–912. [CrossRef]
17. Abo-Khalil, A.G.; Abdelkareem, M.A.; Sayed, E.T.; Maghrabie, H.M.; Radwan, A.; Rezk, H.; Olabi, A.G. Electric vehicle impact on energy industry, policy, technical barriers, and power systems. *Int. J. Thermofluids* **2022**, *13*, 100134. [CrossRef]
18. Lin, S.; He, Z.; Zang, T.; Qian, Q. Impact of plug-in hybrid electric vehicles on distribution systems. In Proceedings of the 2010 International Conference on Power System Technology, Hangzhou, China, 24–28 October 2010; pp. 1–5.
19. Kumar, R.; Saxena, D. Fault analysis of a distribution system embedded with plug-in electric vehicles. In Proceedings of the 2017 Recent Developments in Control, Automation & Power Engineering (RDCAPE), Noida, India, 26–27 October 2017; pp. 230–234.
20. Saleh, S.A.; Ozkop, E.; Valdes, M.E.; Yuksel, A.; Haj-ahmed, M.A.; Sanchez, Z.; Mardegan, C.S. On The Factors Affecting Battery Unit Contributions to Fault Currents in Grid-connected Battery Storage Systems. *IEEE Trans. Ind. Appl.* **2022**, *58*, 3019–3028.
21. IEEE. *IEEE 946–2020—IEEE Recommended Practice for the Design of DC Power Systems for Stationary Applications*; IEEE: Piscataway, NJ, USA, 2020.
22. IEEE. *IEEE Guide for the Protection of Stationary Battery Systems*; Institute of Electrical and Electronics Engineers: New York, NY, USA, 1998.
23. IEEE. *IEEE Recommended Practice for Conducting Short-Circuit Studies and Analysis of Industrial and Commercial Power Systems*; Institute of Electrical and Electronics Engineers: New York, NY, USA, 2018.
24. Wang, L.; Qin, Z.; Slangen, T.; Bauer, P.; Van Wijk, T. Grid impact of electric vehicle fast charging stations: Trends, standards, issues and mitigation measures-an overview. *IEEE Open J. Power Electron.* **2021**, *2*, 56–74.
25. Shaukat, N.; Khan, B.; Ali, S.; Mehmood, C.; Khan, J.; Farid, U.; Majid, M.; Anwar, S.; Jawad, M.; Ullah, Z. A survey on electric vehicle transportation within smart grid system. *Renew. Sustain. Energy Rev.* **2018**, *81*, 1329–1349.
26. Falvo, M.C.; Sbordone, D.; Bayram, I.S.; Devetsikiotis, M. EV charging stations and modes: International standards. In Proceedings of the 2014 International Symposium on Power Electronics, Electrical Drives, Automation and Motion, Ischia, Italy, 18–20 June 2014; pp. 1134–1139.
27. Yilmaz, M.; Krein, P.T. Review of battery charger topologies, charging power levels, and infrastructure for plug-in electric and hybrid vehicles. *IEEE Trans. Power Electron.* **2012**, *28*, 2151–2169.
28. Su, J.; Lie, T.T.; Zamora, R. Integration of Electric Vehicles in Distribution Network Considering Dynamic Power Imbalance Issue. *IEEE Trans. Ind. Appl.* **2020**, *56*, 5913–5923. [CrossRef]
29. Jaramillo Serna, J.d.J.; López-Lezama, J.M. Alternative Methodology to Calculate the Directional Characteristic Settings of Directional Overcurrent Relays in Transmission and Distribution Networks. *Energies* **2019**, *12*, 3379. [CrossRef]
30. Saldarriaga-Zuluaga, S.D.; López-Lezama, J.M.; Muñoz-Galeano, N. Optimal coordination of over-current relays in microgrids considering multiple characteristic curves. *Alex. Eng. J.* **2021**, *60*, 2093–2113. [CrossRef]
31. Clarke, A.D.; Bihani, H.A.; Makram, E.B.; Corzine, K.A. Analysis of the impact of different PEV battery chargers during faults. *J. Power Energy Eng.* **2014**, *2014*, 8. [CrossRef]
32. Jaramillo Serna, J.d.J.; López-Lezama, J.M. Calculation of Distance Protection Settings in Mutually Coupled Transmission Lines: A Comparative Analysis. *Energies* **2019**, *12*, 1290. [CrossRef]
33. Saldarriaga-Zuluaga, S.D.; López-Lezama, J.M.; Muñoz-Galeano, N. Adaptive protection coordination scheme in microgrids using directional over-current relays with non-standard characteristics. *Heliyon* **2021**, *7*, e06665. [CrossRef]
34. Saldarriaga-Zuluaga, S.D.; López-Lezama, J.M.; Muñoz-Galeano, N. An Approach for Optimal Coordination of Over-Current Relays in Microgrids with Distributed Generation. *Electronics* **2020**, *9*, 1740. [CrossRef]
35. IEEE. *IEEE Recommended Practice for Protection and Coordination of Industrial and Commercial Power Systems: Approved September 19, 1985, Reaffirmed June 27, 1991 IEEE Standards Board: Approved February 28, 1986, Reaffirmed December 9, 1991, American National Standards Institute*; IEEE: Piscataway, NJ, USA, 1986.
36. Al-Roomi, A.R. *Optimal Coordination of Power Protective Devices with Illustrative Examples*; John Wiley & Sons: Hoboken, NJ, USA, 2021.

37. Belbachir, N.; Zellagui, M.; Settoul, S.; El-Bayeh, C.Z. Multi-objective optimal renewable distributed generator integration in distribution systems using grasshopper optimization algorithm considering overcurrent relay indices. In Proceedings of the 2021 9th International Conference on Modern Power Systems (MPS), Cluj-Napoca, Romania, 16–17 June 2021; pp. 1–6.
38. Zeineldin, H.H.; Mohamed, Y.A.R.I.; Khadkikar, V.; Pandi, V.R. A protection coordination index for evaluating distributed generation impacts on protection for meshed distribution systems. *IEEE Trans. Smart Grid.* **2013**, *4*, 1523–1532. [CrossRef]
39. Khanbabapour, S.; Golshan, M.H. Synchronous DG planning for simultaneous improvement of technical, overcurrent, and timely anti-islanding protection indices of the network to preserve protection coordination. *IEEE Trans. Power Deliv.* **2016**, *32*, 474–483. [CrossRef]
40. Kar, S.; Samantaray, S.; Zadeh, M.D. Data-mining model based intelligent differential microgrid protection scheme. *IEEE Syst. J.* **2015**, *11*, 1161–1169. [CrossRef]
41. Saldarriaga-Zuluaga, S.D.; López-Lezama, J.M.; Muñoz-Galeano, N. Optimal Coordination of Over-Current Relays in Microgrids Using Unsupervised Learning Techniques. *Appl. Sci.* **2021**, *11*, 1241. [CrossRef]
42. Saad, S.M.; El-Naily, N.; Mohamed, F.A. A new constraint considering maximum PSM of industrial over-current relays to enhance the performance of the optimization techniques for microgrid protection schemes. *Sustain. Cities Soc.* **2019**, *44*, 445–457. [CrossRef]
43. El-Naily, N.; Saad, S.M.; Hussein, T.; Mohamed, F.A. A novel constraint and non-standard characteristics for optimal over-current relays coordination to enhance microgrid protection scheme. *IET Gener. Transm. Distrib.* **2019**, *13*, 780–793. [CrossRef]
44. Saldarriaga-Zuluaga, S.D.; López-Lezama, J.M.; Muñoz-Galeano, N. Optimal coordination of overcurrent relays in microgrids considering a non-standard characteristic. *Energies* **2020**, *13*, 922. [CrossRef]